

## DYNAMIC DESIGN ANALYSIS FOR ROCKFILL DAMS

K. BABA

### SUMMARY

The paper presents a procedure of the dynamic design analysis of rockfill dams. The dynamic behaviors of rockfill dams during strong motion earthquakes show the nonlinear characteristics. These nonlinear phenomena are discussed using analytical results of earthquake observation records on actual rockfill dams, full scale vibration tests by exciter, vibration failure tests of model scale embankments by large shaking table and material tests by cyclic loading apparatus. Those results are available as input data to numerical design analysis that was developed by author et al., and the safety factor could be discussed in a new concept.

### INTRODUCTION

The dynamic behaviors of rockfill dams during earthquakes are still not understood clearly, but recent developments of the investigations for them make more reasonable design procedures and reliable construction performances for rockfill dam.

The earthquake observation on the dam structure and surrounding foundation is preliminary but important step to obtain the vibration behaviors, and the mechanism of their dynamic behaviors are solvable by means of dynamic materials tests under cyclic loading and scale model embankments tests on shaking table. These approaches can assume even a failure mechanism of rockfill dam structure.

These analytical results are input to numerical design analysis under strong motion earthquake, and the results are compared with the results of the preliminary design analysis by conventional methods. The numerical design analysis which is developed by author et al. has some points of expressions for dynamic characteristics of materials, for safety factor by mobilized plane as slip circle as conventional methods.

### VIBRATION CHARACTERISTICS OF ROCKFILL DAM

Earthquake observation on dams is one of the most fundamental and important factors that must be taken into consideration in our design of dams of aseismic structure. Especially the observed records of whole structure indicate the vibration characteristics fairly precisely. Fig. 1 shows the arrangement of seismographs installed on the KUZURYU Dam which was completed in 1974. A rockfill dam of the inclined impervious core type, 128 m high, 355 m in crest length and  $6.3 \times 10^6 \text{m}^3$  in volume and reservoir storage capacity of  $353 \times 10^6 \text{m}^3$  for 220 MW power generation.

---

Kyohei BABA, Director, Engineering Laboratory,  
Electric Power Development Co., Ltd. Japan

With its site located no more than dozens of kilometers away from an active tectonic zone in central Japan, this dam has been subject to earthquakes with a magnitude of between four and seven, and with an epicentral distance of 40 - 50 km in general, at the rate of about once every several years. Fig. 2 shows the accelerograms recorded in 1969 when an earthquake with magnitude 6.6 and an epicentral distance of 40 km hit the dam these accelerograms, which seem to indicate the behavior of a dam during earthquake that is of much interest, are introduced in the following. The No.1 through No.14 accelerograms are those recorded at four points on the dam and on the rock of the left bank, by the use of three-component seismographs. These records indicated the following. First, the No.1 through No.3 for the dam crest each show a fairly predominant peak, 2.4 Hz for the dam axis direction, 2.0 Hz for the river flow direction and 3.7 Hz for the vertical direction. As for the impervious core (No.7 through No.14), the records at higher elevations each showed a predominant peak, while those records at lower elevation showed several peaks similar to those recorded on the rock of both banks. The No.4 through No.6 recorded on the rock of the left bank showed a predominant peak at nearly 1.0 Hz, also showing another predominant peak at almost 5 Hz. These results clearly show that the input at the foundation rock, though it contains wide-ranging vibration components to some extent, led to the response of the dam which is characterized by remarkably predominant vibration period. This fact seems to indicate that the response of the dam predominantly shows a natural vibration period, irrespective of short period components contained in the input. Also, it was found that the predominant period of the dam tend to become shorter in relation to the river flow direction, dam axis direction and the vertical direction in that order. In addition, this predominant period was found representing the 1st order, the 2nd order or higher order period.

On the other hand, a full scale vibration tests by exciter can obtain a vibration modes and natural periods. But those are only enough to know them, because the vibration force is extremely small, that is, the structure vibrates in an elastic range.

So the vibration failure test of scale model embankment are possible to obtain a failure mechanism of embankment during strong vibrations not only to obtain a vibration characteristics within elastic range.

In the case of the failure tests of the embankment which are composed of crushed stones (average diameter; 25 cm, total weight of embankment; 110 ton), the studies pursued 3 types of embankments; homogeneous, embankment on soft foundation and mixed size of crushed stones. It was founded that the surface stones of the homogeneous embankment slipped and sunked down, the upper part of the embankment on soft foundation vibrated extremely than other part and the large stones of the surface of the mixed size embankment slipped down as on the slide made by sunked small size stones. these facts suggest a design feature for outer zone of rockfill dam.

DYNAMIC NUMERICAL ANALYSIS

On the basis of the results so far obtained, it will be now supposed to formulate each step necessary for numerical analysis. Here, some of the items that seem to have important effects on the outcome of numerical analysis are discussed as follow.

The first item concerns how the physical property values should be expressed. As far as core material is concerned, measurement was taken by means of a geophysical exploration method of the distribution of S-wave velocity and P-wave velocity to determine a velocity distribution model so that the results of earthquake observation may be compared with the above model. Then, considering the fact that the ratio of stress within an embankment under construction to principal stress can be considered constant, and that some 70% of the load on the core can be considered, the average effective principal stress  $\sigma'_m$ , the shearing elasticity  $G_0$  and Poisson's ratio  $\nu$  are expressed as follows.

$$\begin{aligned} \sigma'_m &= 0.3 (1 + \nu)\rho_z \\ G_0 &= \rho v_s^2 = \rho(140Z^{0.34})^2 \dots\dots\dots (1) \end{aligned}$$

$$\begin{aligned} \nu &= 0.45 - 0.006Z^{0.60} \\ G_0 &= 2,168 (\sigma'_m)^{0.69} \dots\dots\dots (2) \end{aligned}$$

here, Z: depth below surface

Fig. 5 shows the relations as expressed in the equation above. The equation (2) is for micro-strain amplitude. On the other hand, on the basis of the results of dynamic triaxial material tests, there is proportional relation between  $\sigma'_m$  and the dynamic secant modulus (Fig. 6). Therefore, after determining, Poisson's ratio taking into account the void ratio reliance of  $G_0$ 's, the dynamic shearing modulus G for core material is expressed as follows,

$$G = 395 \frac{(2.97 - e)^2}{1 + e} \cdot \frac{1}{1 + \frac{\gamma}{1.33 \times 10^{-4}}} (\sigma'_m)^{0.69} \dots\dots\dots (3)$$

Similarly, the results of dynamic triaxial material tests conducted on rock material provide the relations. Therefore, the following equation is obtained.

$$G = 440 \frac{(2.97 - e)^2}{1 + e} \cdot \frac{1.56 \times 10^3}{1.56 \times 10^{-3} + \gamma} (\sigma'_m)^{0.55} \dots\dots\dots (4)$$

As for the damping factor  $h$ , the following equation is formulated, taking into consideration the results of dynamic triaxial tests and various seismograms, and assuming the radiation damping factor to be 15% on the basis of various seismograms, multireflection and exciter test results.

$$h = 0.23 \frac{\gamma}{\gamma + 1.33 \times 10^{-4}} + 0.15 \dots\dots\dots (5)$$

However, the equation above are required to be corrected on the basis of the results to be obtained by conducting further material tests, vibration tests, etc. and by making further earthquake observations, so that they may hold good for higher levels of strain.

To make a final evaluation of the numerical analysis, it is obtained a shearing stress in the mobilized plane with regard to elements with a safety factor of less than 1, so that, when the plane formed through connection of these direction of shearing stress in the elements goes out the embankment body, it may be obtained a macro-slip safety factor regarding the plane thus formed as a slip plane (Fig. 7).

#### CONCLUSION

The dynamic behaviors of rockfill dams during earthquakes have so far discussed on the basis of the results of earthquake observations and experimental studies, also introducing an example of a numerical analysis made of these results.

In a practical design procedure, the relationships of the safety factor between conventional analysis and above mentioned analysis are obtained.

Fig. 8 shows the relation curve of design seismic factors which are statical seismic factor for conventional method and design acceleration for a dynamic analytical method, at the case of same value of safety factor respectively. The relation curve suggests many meanings for the development of more practical design method.

#### REFERENCES

1. ON A CONSIDERATION FOR AN EARTHQUAKE-RESISTANT DESIGN METHOD FOR ROCKFILL DAMS  
K. BABA, H. WATANABE                                      Q51 R15 ICOLD, 1979
2. Dynamic behaviour of rockfill dams  
M. NOSE, K. BABA    Design of dams to resist earthquake ICE, London, 1980

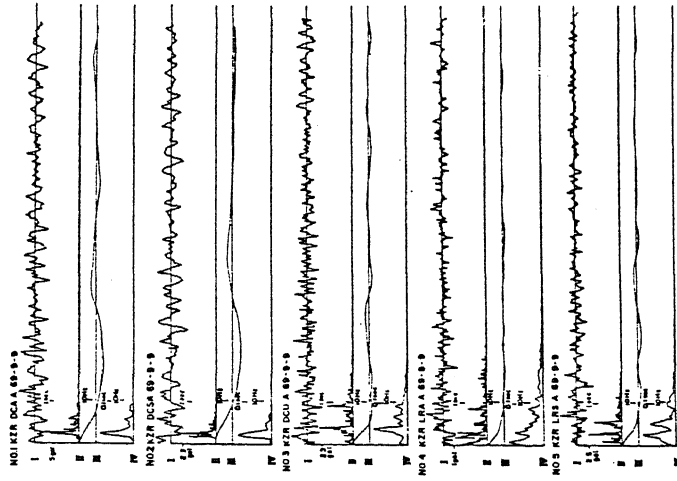


Fig. - 2 Earthquake Record on KUZURYU DAM

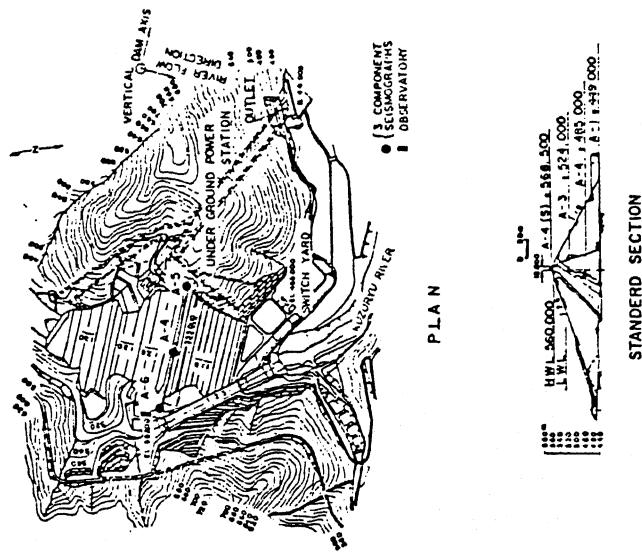


Fig. 1 Arrangement of Seismographs on KUZURYU Dam

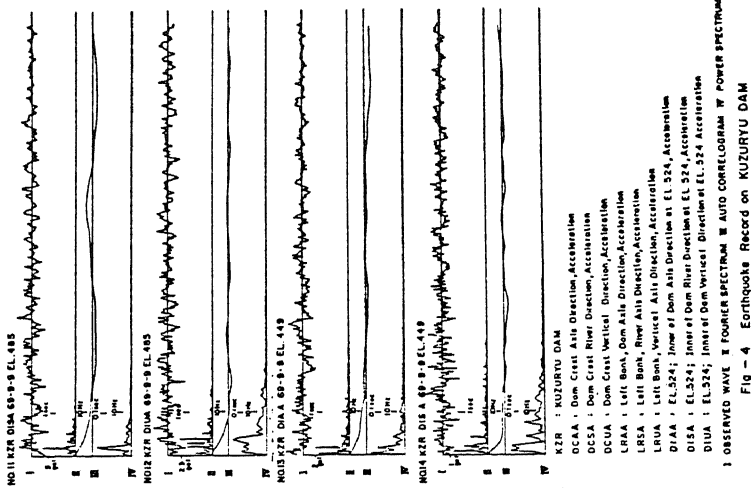


Fig - 3 Earthquake Record on KUZURYU DAM

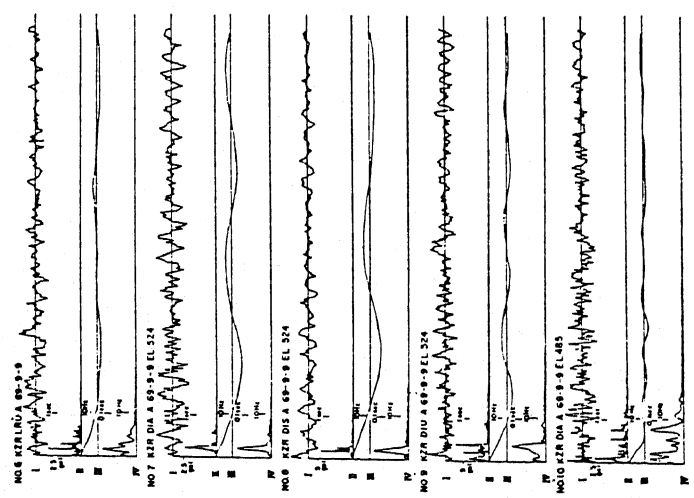


Fig - 4 Earthquake Record on KUZURYU DAM

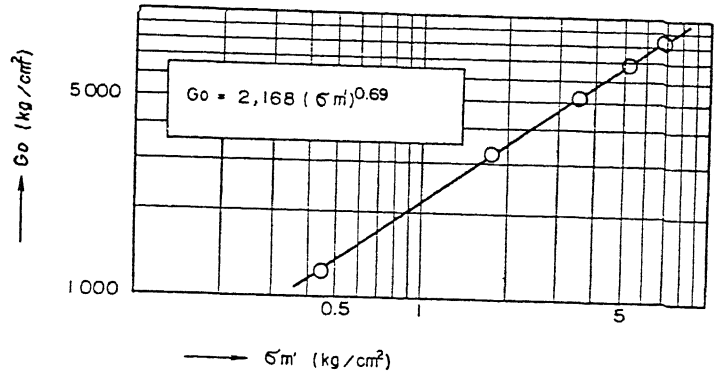


Fig. 5  $G_o \sim \sigma_{m'}$  Relation for Core Material

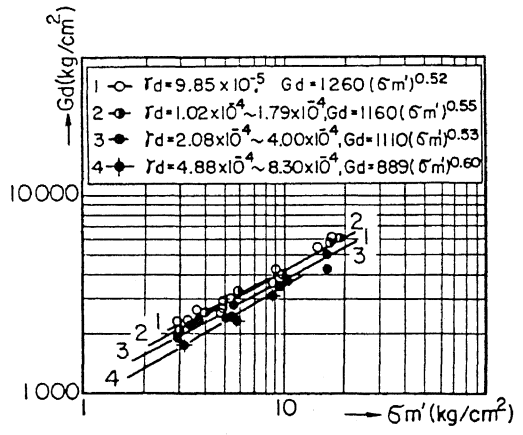


Fig. 6  $G_d \sim \sigma_{m'}$  Relation

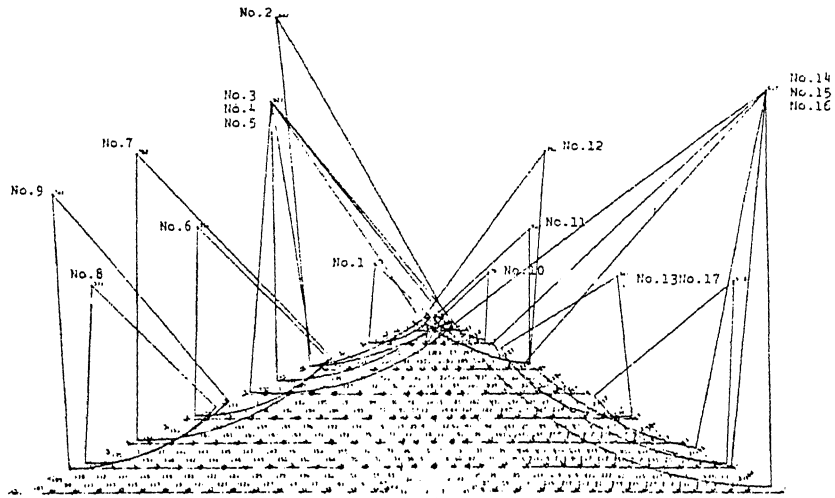


Fig.7 Representative Potential Sliding Circle

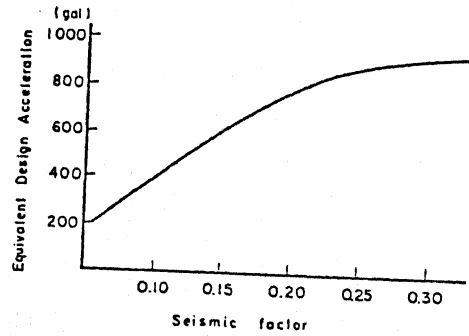


Fig.8 Relationship between static factor and Acceleration (Baba.K)